Earth and Planetary Science Letters 355-356 (2012) 51–59

Contents lists available at SciVerse ScienceDirect

Earth and Planetary Science Letters

journal homepage: www.elsevier.com/locate/epsl

Riverine particulate material dissolution as a significant flux of strontium to the oceans

Morgan T. Jones [a,*], Christopher R. Pearce [b,1], Catherine Jeandel [c], Sigurður R. Gislason [a], Eydis S. Eiriksdottir [a], Vasileios Mavromatis [b], Eric H. Oelkers [a,b]

[a] Institute of Earth Science, University of Iceland, Sturlugata 7, 101 Reykjavík, Iceland
[b] Géoscience-Environnement Toulouse (GET), UMR CNRS 5563, Université Paul-Sabatier, Observatoire Midi-Pyrénées, 14 avenue Edouard Belin – 31400 Toulouse, France
[c] Laboratoire d'Etudes en Géophysique et Océanographie Spatiale (LEGOS), UMR CNRS 5566, Université Paul-Sabatier, Observatoire Midi-Pyrénées, 14 avenue Edouard Belin – 31400 Toulouse, France

ARTICLE INFO

Article history:
Received 3 February 2012
Received in revised form
31 July 2012
Accepted 22 August 2012
Editor: G. Henderson

Keywords:
strontium isotopes
riverine particulate material
seawater composition
marine mass balance

ABSTRACT

The ratio of strontium isotopes, $^{87}Sr/^{86}Sr$, in seawater is homogenous at any given time, yet varies considerably throughout the geological record. This variation is thought to stem from changes in the balance of predominantly radiogenic Sr entering the oceans via dissolved riverine transport, and unradiogenic Sr sourced from mid-ocean ridge hydrothermal activity. Recent evidence suggests, however, that hydrothermal exchange at mid-ocean ridges is a factor of 3 too low to balance Sr added to the oceans from dissolved continental riverine fluxes. Here we present evidence that the arrival and subsequent dissolution of riverine particulate material in seawater is a significant contributor of both radiogenic and unradiogenic Sr to the oceans. Batch experiments demonstrate that between 0.15% and 27.36% of Sr is liberated from riverine particulates to seawater within 6 months. The rates of release are dependent on surface area and particulate composition, with volcanic riverine material more reactive than continental riverine particulates. The observed rapid Sr release rate from riverine particulate material has important consequences for both chemical and isotopic mass balances in the ocean and the application of the $^{87}Sr/^{86}Sr$ weathering proxy to the geological record. The dissolution of riverine particulate material is likely, based on these findings, to at least partially account for the imbalance between Sr sources to the oceans.

1. Introduction

The riverine transport of elements from the continents to the oceans is a major process in the global cycling of elements (Martin and Meybeck, 1979; Milliman, 2001; Gaillardet et al., 2003). This process plays a critical role in climate regulation and nutrient transport within global biogeochemical cycles. Rivers carry elements in both dissolved and particulate form, the latter a product of mechanical weathering and the growth/decay of organic material. The dissolved riverine flux has been the focus of many scientific studies, significantly more than studies concentrating on the particulate flux (Gislason et al., 2006). The best estimates for the global dissolved riverine flux are approximately 1 Gt yr^{-1} (Gaillardet et al., 1999, 2003; Viers et al., 2009), while the suspended flux is at least an order of magnitude greater at 15–20 Gt yr^{-1} (Meybeck et al., 2003; Syvitski et al., 2003; Walling, 2006; Peucker-Ehrenbrink et al., 2010). If the bedload transported component is included, this particulate flux may be as high as 16.6–30 Gt yr^{-1} (Walling, 2006). Therefore, particulate fluxes dominate over dissolved fluxes for the majority of elements, particularly insoluble elements such as Al, Ti, Fe, and Zr (Oelkers et al., 2011; Jones et al., 2012). If a significant proportion of this particulate material dissolves or undergoes ion exchange with ocean seawater, then the riverine particulate flux may be an important contribution of various radiogenic and stable isotope systems in the world's oceans. The degree to which riverine particulate matter plays a role in the compositional evolution of seawater depends on the reactivity of each element after the particle's arrival in the ocean. The use of isotope ratios is a valuable method of deciphering sediment – water interaction, which is crucial to constrain the current understanding of ocean circulation, biological production, and element cycling (e.g. Tipper et al., 2006; Vance et al., 2009; Hsieh et al., 2011; Jeandel et al., 2011).

The interpretation of various biogeochemical and element cycles are often based on the assumption that dissolved riverine isotopic compositions are conservatively transferred to the ocean. However, deltas and estuaries act as fluidized bed reactors that

* Corresponding author. Tel.: +354 525 4495.
E-mail address: morgan@hi.is (M.T. Jones).
[1] Present address: Department of Earth and Environmental Sciences, The Open University, Walton Hall, Milton Keynes, MK7 6AA, United Kingdom.

0012-821X/$ - see front matter © 2012 Elsevier B.V. All rights reserved.
http://dx.doi.org/10.1016/j.epsl.2012.08.040

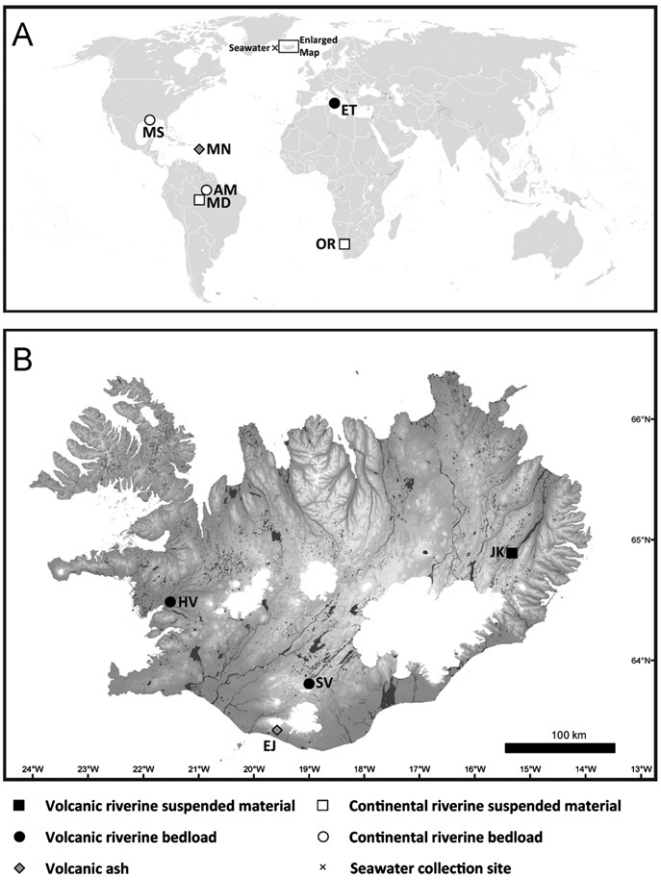

Fig. 1. (A) Map of the world showing sample locations. (B) Map of Iceland showing water bodies and sample locations. Sample site labels: MS=Mississippi, MN=Montserrat, AM=Amazon, MD=Madeira, OR=Orange, ET=Etna, HV=Hvítá, SV=Sveinsgil, JK=Jökulsá í Fjótsdal, EJ=Eyjafjallajökull.

rework sediments for months after arrival from continental sources (Aller, 1998), and various interactions between deposited particulate material and saline water have been identified in estuarine and deltaic systems (Mackenzie and Garrels, 1966; Michalopoulos and Aller, 1995; Aller et al., 2008). Moreover, field measurements of Li, Mo, and U isotopes in estuarine waters suggest that isotopic fractionation may be caused by interactions between the particulate and liquid phases (Pogge von Strandmann et al., 2008; Pearce et al., 2010). Particulate matter dissolution has also been shown to play a significant role in transporting Nd to the oceans (Lacan and Jeandel, 2005; Arsouze et al., 2009). Moreover, it has been suggested that the particulate flux of Ca that subsequently dissolves in seawater is comparable in magnitude to that derived from the dissolved riverine flux (Gislason et al., 2006, Wallmann et al., 2008). Therefore, the assumption of conservative transfer between rivers and oceans, both for dissolved and particulate material, must be questioned.

Experimental evidence has recently shown that the isotopic ratio of radiogenic ^{87}Sr and stable ^{86}Sr in seawater can be significantly altered when in contact with basaltic riverine particulate material (Jones et al., 2012). Seawater reacting with the particulate material displayed little change in Sr concentrations, yet mass balance calculations based on the observed change in liquid $^{87}Sr/^{86}Sr$ indicated that over 3% of the original Sr in riverine bedload collected from the Hvítá River (Iceland) was released during 9 months of reaction. These results indicate a significant two-way flux of Sr between solid and liquid phases that are of a similar magnitude. Whether this process is dominated by the dissolution of primary material and the precipitation of secondary phases and/or ion exchange is not clear, but the net result is the effective masking of this coupled process from detection by total element concentration measurements. Estuarine sediment sampled from the same catchment had a negligible effect on seawater $^{87}Sr/^{86}Sr$, suggesting that these reactions occur when particulate material first arrives into coastal waters (Jones et al., 2012).

The ratio of $^{87}Sr/^{86}Sr$ in seawater is currently homogenous at 0.70916 owing to the ~2.3 Ma residence time of Sr in the ocean (e.g. Broecker and Peng, 1982). The traditionally accepted primary inputs of Sr to the oceans are Sr entering the oceans via dissolved riverine transport with $^{87}Sr/^{86}Sr \approx 0.7136$ (Vance et al., 2009; Allègre et al., 2010), and Sr exchange from mid-ocean ridge hydrothermal activity with $^{87}Sr/^{86}Sr \approx 0.7029$ (Albarède et al., 1981). Another significant flux is through groundwater transport, although this is poorly constrained (Allègre et al., 2010). The dissolved riverine flux is a combination of dissolution products of evolved continental catchments, with an $^{87}Sr/^{86}Sr$ generally elevated with respect to seawater, and sub-aerial volcanic sources with an $^{87}Sr/^{86}Sr$ typically between 0.7030 and 0.7060 (Goldstein and Jacobsen, 1987). The estimated dissolved Sr is approximately 16.5×10^{11} g yr^{-1} (Gaillardet et al., 1999), while the Sr transported in particulates is about a factor of two larger (Oelkers et al., 2011). The exchange/dissolution of 3% Sr in the Hvítá riverine bedload experiments (Jones et al., 2012) suggests that the riverine particulate flux could be an important input of Sr to the oceans. However, Sr release from riverine particulates is likely to vary considerably between geological settings, climate, and many other factors. It is therefore important to characterize how particulate materials from a variety of rivers behave in seawater. This study characterizes the controls of riverine particulate material as in input of Sr to the oceans through the direct measurements of changes to seawater compositions in response to mixing with riverine particulate material collected from a variety of sources located throughout the world.

2. Materials and methods

Closed-system experiments were performed on selected samples to assess Sr release rates in seawater. Ten distinct particulate matter samples were considered. The sample localities are shown in Fig. 1A and B. Four riverine particulate samples were collected from volcanic terrains, four riverine samples were sampled from continental catchments, and two fresh volcanic ashes were collected immediately after eruptions. The sample locations are as follows:

Continental riverine samples:

(1) A composite sample consisting of a 5:1 bedload material to suspended particulate material ratio was collected from the main part of the Amazon River in South America. The sample was collected in March 2006 in the town of Parintins and is labeled "AM" in each figure.
(2) A suspended material sample was collected from the Madeira River catchment of the Amazon basin in March 2006 near the town of Porto Velho. The sample was collected at a depth of 7 m and 1.6 km from the left bank. The sample locality is labeled "MD" in the figures.
(3) A bedload material sample from the Mississippi River in North America was collected in western New Orleans in July 2010. The sample was collected below the water line on the northern bank and is labeled "MS" in each figure.
(4) A mud bank deposit was collected from the Orange River in southern Africa. This sample has been previously characterized

by Compton and Maake (2007) and is labeled "OR" in the figures.

Volcanic riverine samples:

(5) Bedload material from the Hvítá River in western Iceland was collected from a sandbank adjacent to the river. This is the same sample as used in Jones et al. (2012), and the river is a mix between spring, glacial and meteoric sources. It is labeled as "HV" in the figures.

(6) A suspended riverine material was obtained from the Jökulsá í Fljótsdal River in north-east Iceland. The catchment is dominantly basaltic, and the riverine particulate material is dominated by tilled material originating from the Vatnajökull icecap. The sample was collected by filtering 60 L of river water using a Sartorius® tangential filtration unit and a Hydrosart® 0.2 μm filtration cartridge. The slurry was centrifuged for 10 min at 15 °C at 10,000 rpm, and the remaining solids were freeze dried for 24 h in at −40 °C and 0.21 bar pressure (Eiriksdottir et al., 2008; Gislason et al., 2008). The sample is labeled as "JK" in each figure.

(7) A bedload material sample was collected from a sandbank adjacent to the Sveinsgil tributary of the Tungnaá River in south-central Iceland. This tributary is completely within the rhyolitic caldera associated with the Torfajökull volcano, but is the only intra-caldera tributary with a minimal geothermal component. The sample is labeled "SV" in each figure.

(8) A bedload sample was collected from the Salaro river bed on the eastern flanks of Etna volcano in Sicily, just uphill from the town of Zafferana Etnea. Much of the drainage basin just uphill from this sample site is covered by lava erupted in 1792, although the sample site itself is densely vegetated and has substrate older than historical times (< 14th Century). The sample is labeled "ET" in the figures

Volcanic ash samples:

(9) Fresh, unhydrated volcanic ash was collected during the eruption of Eyjafjallajökull in April 2010. This sample was previously characterized by Gislason et al. (2011) and is labeled "EJ" in the figures.

(10) Fresh, unhydrated volcanic ash was collected during an eruption from the Soufrière Hills volcano, Montserrat, following the large dome collapse event in 2003. This sample was previously characterized by Jones and Gislason (2008) and is labeled as "MN" in the figures.

The sampling locations, major element data, $^{87}Sr/^{86}Sr$ ratios, and BET (Brunauer, Emmett and Teller method; Brunauer et al., 1938) specific surface area of these samples are given in Table 1. The samples were either collected dry or freeze dried once all excess liquid had been removed. No other processing was done prior to the experiments. Surface seawater used in these experiments was collected to the west of Iceland at the Faxaflói 9 station at a depth of 3 m in February 2011 (64°20′ N and 27°58′ W, Fig. 1A). This surface seawater does not have a significant riverine input, allowing the clear identification of any particulate–liquid interaction. The water was tangential filtered using a 0.2 μm cellulose acetate membrane filter then acidified to pH 2 using 7 M HCl and was subsequently stored in the dark. Prior to commencing the experiments the pH was re-equilibrated to 8.1 at 21 °C using 1 M NaOH.

The closed-system experiments were performed by mixing the various particulate samples with the collected seawater in a clean laboratory at room temperature. Each experiment had approximately 1:3 particulate to seawater ratio by weight; the total volumes varying depending on the amount of particulate material available (see Appendix A). All experiments were performed in polypropylene batch reactors fixed to a Heidolph Vibramax 100

Table 1
Sample locations, BET surface areas, $^{87}Sr/^{86}Sr$, and major element compositions of the samples used in these experiments. The compositions of the volcanic ashes were measured in Jones and Gislason (2008) and Gislason et al. (2011). The errors for BET measurements were ±10% according to in-house standards.

	Continental rivers					Volcanic rivers				Volcanic ash	
Type	Bedload	Bedload	Composite	Suspended	Bedload	Bedload	Bedload	Suspended		
Name	Mississippi	Orange	Amazon	Madeira	Etna	Sveinsgil	Hvítá	Jökulsá	Montserrat	Eyjafjallajökull
Latitude	29°55′15″ N	28°45′58″ S	2°36′20″ S	8°40′10″ S	37°42′15″ N	63°57′40″ N	64°32′40″ N	64°59′02″ N	16°44′57″ N	63°31′28″ N
Longitude	090°08′05″ W	017°37′35″ E	056°44′20″ W	063°54′54″ W	015°05′24″ E	019°00′00″ W	021°49′58″ W	015°05′21″ W	062°13′38″ W	019°33′28″ W
BET ($m^2\ g^{-1}$)	3.05	18.23	7.32	11.35	1.49	17.35	6.36	22.26	3.08	9.35
Sr (mg/kg)	152.78	153.67	171.38	184.20	940.44	142.52	152.87	294.39	241.32	291.51
$^{87}Sr/^{86}Sr$	0.715700	0.716474	0.71126	0.73148	0.703604	0.703307	0.70318	0.70330	0.703577	0.703251
SiO_2 (%)	79.25	52.92	71.13	69.77	45.2	59.05	46.74	43.92	61.9	57.98
Na_2O (%)	1.56	2.39	1.81	0.74	5.74	3.21	2.67	3.26	3.86	5.01
MgO (%)	0.51	2.92	0.76	1.11	3.02	1.35	8.17	3.89	2.34	2.30
Al_2O_3 (%)	6.38	18.07	9.84	13.67	19.37	15.23	15.24	15.27	16.37	14.87
P_2O_5 (%)	0.10	0.12	0.09	0.08	0.57	0.24	0.14	0.38	0.15	0.53
K_2O (%)	1.71	1.49	2.26	2.45	1.63	2.15	0.28	1.18	0.92	1.79
CaO (%)	1.34	4.60	1.55	0.41	6.98	2.56	14.02	9.20	6.33	5.50
TiO_2 (%)	0.43	0.78	0.71	0.85	1.39	1.30	1.45	2.62	0.56	1.80
MnO (%)	0.03	0.10	0.05	0.07	0.15	0.12	0.24	0.24	0.15	0.24
Fe_2O_3 (%)[a]	1.39	8.64	3.70	5.61	11.50	9.13	10.81	11.86	6.57	9.75

[a] Denotes total iron.

Platform Shaker, set at 150 rpm. This setting was chosen to allow liquid mixing while not disturbing the particulate–water interface. These experiments ran for 6 months and were periodically sampled. All liquids were passed through a 0.45 μm MF-Millipore MCE membrane filter immediately after sampling. The samples were then subdivided for elemental analysis, pH measurement, and isotopic analysis. The removal of samples lowered the liquid volume in the reactors by $\leq 24\%$ at the end of the experiments.

Element analyses for the aliquots were conducted using Spectro Ciros Vision inductively coupled plasma-atomic emission spectroscopy (ICP-AES) in Reykjavík. Uncertainties were ascertained using replicate samples at varying dilutions to account for any effect of Na on the Nebulizer. The error associated with this method did not exceed $\pm 5\%$, except for elements with high initial concentrations such as Na, Mg, and S where errors were up to $\pm 25\%$ due to the effect of Na loading. Samples were run at several dilutions to account for any interference of Na on the plasma. The ratios of $^{87}Sr/^{86}Sr$ were obtained using a MAT 261 thermal ionization mass spectrometer (TIMS) in Toulouse and normalized to an $^{86}Sr/^{88}Sr$ ratio of 0.1194. Eight analyses of the NBS 987 standard had a mean value of 0.710253 ± 0.000014 (2 SD), which compares well with the accepted value of 0.710263 ± 0.000016 (Stein et al., 1997). Individual errors did not exceed ± 0.000016 $^{87}Sr/^{86}Sr$ and blanks of the total analytical procedure showed that Sr contamination was negligible compared to the Sr in the samples.

3. Results

3.1. Impact of dissolution on seawater $^{87}Sr/^{86}Sr$

The $^{87}Sr/^{86}Sr$ evolution of the reacted seawater during all experiments is shown in Fig. 2. Without exception, the particulate materials changed the isotopic composition of Sr in the reacting seawater, with all deviations being significantly greater than the ± 0.000016 analytical error. Much of this $^{87}Sr/^{86}Sr$ change occurs within 24 h. For the particulate material from continental catchments the reaction with seawater resulted in higher measured $^{87}Sr/^{86}Sr$ values than that of original seawater (0.70916), while the riverine particulate material from volcanic terrains and volcanic ash caused the $^{87}Sr/^{86}Sr$ values of the reacting water to decrease. The evaporation of co-sampled interstitial pore-waters can be discounted as the source of this liberated Sr; if a close packed particulate material with 40% porosity and a density of 3 g cm^{-3}, and typical values for dissolved riverine concentrations at each river are assumed, then the observed changes in reacted seawater Sr isotopic compositions are from 112 to 35,800 times too high to originate from residual salt dissolution.

The degree of Sr released to seawater varied considerably between the closed-system experiments (Fig. 2). The reacted seawater $^{87}Sr/^{86}Sr$ values in each of the volcanic particulate experiments continue to decrease after six months, while $^{87}Sr/^{86}Sr$ appears to be nearly constant in the continental particulate experiments after one month. The differences exhibited between experiments can be related to lithology, Sr concentrations, $^{87}Sr/^{86}Sr$ values, and BET surface areas of the samples (see Table 1). This is illustrated in Fig. 3A, which shows the calculated total Sr released from the particulate material, based on the measured change in the $^{87}Sr/^{86}Sr$ ratio of seawater calculated using equations reported by Jones et al. (2012). A large variation between the behaviors of the different particulate materials is evident. At one extreme is the suspended particulate material from Jökulsá í Fljótsdal (JK), which releases 27.3% of its Sr to the liquid phase in six months, while the bedload collected from the river on Etna and from the Mississippi only release 0.15% and 0.2% of the their particulate Sr, respectively, during the experiments. The range for the other seven experiments is between 2.1% and 11.6% Sr released after 6 months. Fig. 3B shows Sr release from the particulate material normalized to BET surface area. This shows a general pattern within the available dataset, where surface area normalized Sr release rates from volcanic ash > volcanic riverine material > continental riverine material. The only exception to this is the Jökulsá í Fljótsdal suspended material, which released

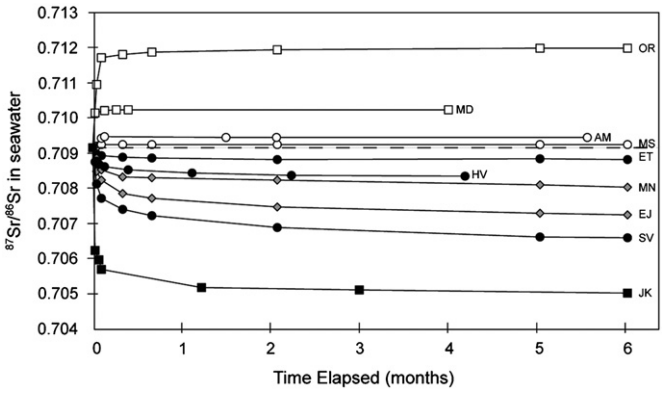

Fig. 2. Measured $^{87}Sr/^{86}Sr$ ratios of seawater after reaction with particulate material of different origin. The dashed line is the $^{87}Sr/^{86}Sr$ of the original seawater. The symbols match those described in Fig. 1.

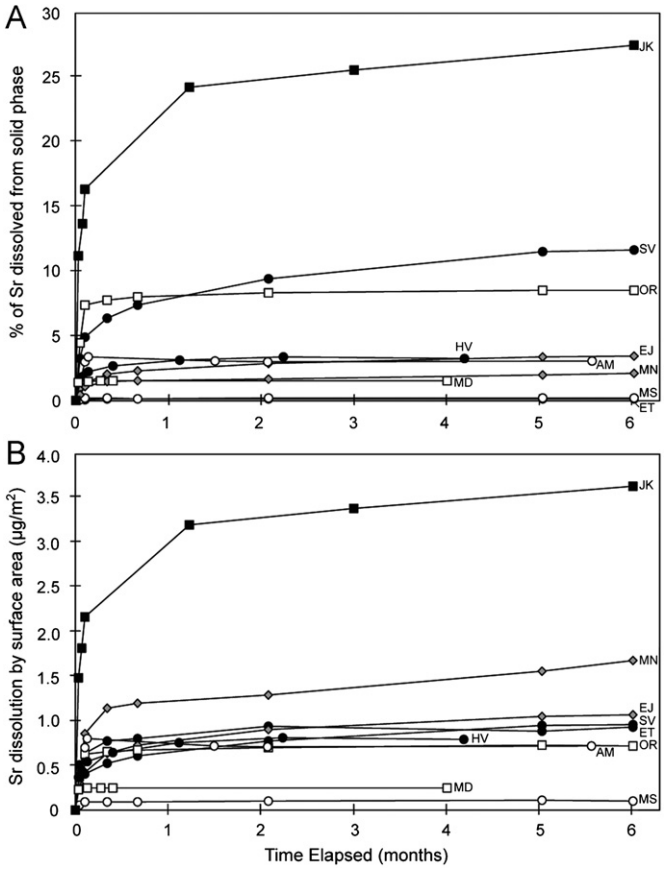

Fig. 3. (A) The percentage of the total Sr present in particulate material released to seawater, based on the measured seawater Sr isotope composition changes. This assumes that the Sr released had the same $^{87}Sr/^{86}Sr$ as the bulk particulate material. (B) The Sr released from the solid phase, normalized to each particle's BET surface area. The symbols match those described in Fig. 1. The calculations and derivations are shown in Appendix A.

considerably more Sr than any of the other experiments, even after factoring its high surface area (see Table 1). At the end of the continental particulate experiments the Sr release is in the range of 0.1–0.71 μg m^{-2}, while the volcanically derived material is in the range of 0.78–3.62 μg Sr m^{-2}. An interesting comparison is the relative behaviors of sediment from Sveinsgil (SV) at Etna (ET). When considering the percentage of Sr released (Fig. 3A), the Sveinsgil experiment displays Sr release nearly 80 times greater than the Etna experiment, yet due to the large differences in surface areas and Sr concentrations of the samples these two experiments display almost identical surface area normalized Sr release rates (Fig. 3B). The same is true when comparing sediments from the Amazon and Orange Rivers, where the surface area normalized release rates are identical despite the Orange River experiment causing the larger shift in seawater $^{87}Sr/^{86}Sr$ (Fig. 2).

3.2. Changes in element concentrations

The dissolved concentrations of selected elements from seven of the experiments are shown in Table 2. Dissolved Si increases from the initial value of 0.22 ppm in all experiments, consistent

Table 2
The changes in pH and certain element concentrations in reacted fluids during the course of selected experiments. The predicted Sr originates from mass balance equations based on the change in $^{87}Sr/^{86}Sr$ (see Appendix A and Jones et al., 2012, for these derivations. Italicized numbers represent concentrations below the instrument detection limit.

Sample Name	Sample Units	Time (months)	pH	Si (mg/kg)	K (mg/kg)	Fe (mg/kg)	Al (mg/kg)	Mn (mg/kg)	Sr (mg/kg)	Predicted Sr (mg/kg)	Pred.–Obs. (mg/kg)
Hvítá	SW	0.00	8.13	0.13	447	*0.00*	0.18	*0.00*	8.85	8.85	0.00
	HV1	0.03	7.18	0.87	402	*0.00*	*0.02*	0.16	8.76	9.48	0.72
	HV2	0.07	6.86	1.24	414	*0.00*	*0.01*	0.22	8.81	9.62	0.81
	HV3	0.13	6.74	1.51	437	*0.00*	*0.00*	0.29	9.41	9.79	0.39
	HV4	0.40	6.66	2.89	431	*0.00*	*0.00*	0.51	9.35	9.97	0.62
	HV5	1.12	6.65	2.45	430	*0.00*	*0.00*	0.88	9.46	10.17	0.71
	HV6	2.24	6.65	2.77	421	*0.00*	*0.01*	1.26	9.26	10.26	1.00
	HV7	4.19	6.77	2.70	408	*0.00*	*0.01*	1.59	8.88	10.23	1.34
Jökulsá	SW	0.00	7.80	0.22	447	*0.00*	*0.01*	*0.00*	6.86	6.86	0.00
	JK1	0.03	7.43	6.92	397	*0.01*	0.12	0.27	15.23	15.63	0.40
	JK2	0.07	7.20	8.21	390	*0.02*	0.10	2.34	16.99	17.55	0.56
	JK3	0.10	6.99	8.40	388	*0.04*	0.12	3.93	19.24	19.64	0.40
	JK4	1.23	6.94	14.29	361	0.08	0.14	4.98	25.08	25.75	0.67
	JK5	3.00	6.89	19.23	345	0.16	0.15	7.01	26.02	26.83	0.81
	JK6	6.02	6.90	22.75	328	0.30	0.15	9.06	27.03	28.31	1.28
Sveinsgil	SW	0.00	7.80	0.22	447	*0.00*	*0.01*	*0.00*	6.86	6.86	0.00
	SV1	0.04	7.31	6.30	320	*0.03*	0.18	10.65	6.86	8.35	1.49
	SV2	0.10	6.55	10.53	360	*0.04*	0.22	14.36	7.99	9.12	1.13
	SV3	0.34	5.40	15.08	374	0.19	0.75	18.13	8.73	9.78	1.05
	SV5	2.08	4.13	35.14	332	33.00	13.38	36.05	8.51	11.20	2.69
	SV7	6.02	3.92	47.40	330	42.97	22.01	45.31	9.91	12.23	2.32
Etna	SW	0.00	7.80	0.22	447	*0.00*	*0.01*	*0.00*	6.86	6.86	0.00
	ET1	0.04	8.01	1.38	402	*0.04*	0.46	0.02	7.18	7.10	−0.08
	ET2	0.10	7.92	2.15	408	*0.00*	0.14	0.24	7.53	7.16	−0.37
	ET3	0.34	7.77	3.08	384	*0.01*	0.13	1.30	7.07	7.23	0.16
	ET5	2.08	7.95	3.54	364	*0.01*	0.02	0.40	6.79	7.30	0.52
	ET7	6.02	7.76	3.56	373	*0.00*	0.12	0.04	7.26	7.30	0.04
Orange	SW	0.00	7.80	0.22	447	*0.00*	*0.01*	*0.00*	6.86	6.86	0.00
	OR1	0.04	7.75	5.51	275	*0.01*	0.07	0.99	7.79	9.09	1.30
	OR2	0.10	7.49	9.58	244	*0.00*	0.08	1.85	8.40	10.56	2.17
	OR3	0.34	7.46	12.50	229	*0.01*	0.13	2.61	8.15	10.76	2.61
	OR5	2.08	7.33	15.23	217	*0.00*	*0.00*	*0.01*	8.23	11.04	2.81
	OR7	6.02	7.15	16.74	285	*0.00*	*0.00*	*0.01*	8.96	11.15	2.18
Mississippi	SW	0.00	7.80	0.22	447	*0.00*	*0.01*	*0.00*	6.86	6.86	0.00
	MS1	0.04	7.81	1.26	375	*0.00*	0.27	0.01	7.04	6.91	−0.13
	MS2	0.10	7.64	1.80	374	*0.03*	0.11	0.02	7.05	6.95	−0.10
	MS3	0.34	7.58	2.35	391	*0.00*	0.12	0.12	7.25	6.95	−0.30
	MS5	2.08	7.49	2.86	354	*0.00*	*0.01*	1.89	6.83	6.95	0.12
	MS7	6.02	7.34	3.10	346	*0.00*	*0.00*	2.00	7.13	6.96	−0.17
Eyjafjallajökull	SW	0.00	7.80	0.22	447	*0.00*	*0.01*	*0.00*	6.86	6.86	0.00
	EJ1	0.04	7.92	5.97	385	*0.02*	0.03	0.51	7.57	7.76	0.20
	EJ2	0.10	8.02	7.87	393	*0.00*	0.04	0.48	8.24	8.14	−0.10
	EJ3	0.34	8.14	8.76	330	*0.03*	0.08	0.33	7.32	8.79	1.47
	EJ4	0.67	8.10	9.94	367	0.05	0.11	0.32	7.45	9.07	1.62
	EJ5	2.08	8.10	11.43	312	*0.00*	*0.00*	0.28	7.23	9.60	2.37
	EJ7	6.02	8.07	13.21	309	*0.00*	*0.02*	0.31	8.07	10.12	2.05
Montserrat	SW	0.00	7.80	0.22	447	*0.00*	*0.01*	*0.00*	6.86	6.86	0.00
	MN1	0.04	6.49	2.96	355	*0.00*	0.04	15.57	6.61	7.24	0.63
	MN2	0.10	6.40	8.46	384	1.82	4.39	37.64	7.74	7.75	0.01
	MN3	0.34	4.92	20.20	373	10.93	9.22	47.34	7.65	8.05	0.41
	MN5	2.08	4.00	72.25	309	41.01	43.53	44.95	4.41	8.20	3.79
	MN7	6.02	3.39	89.80	386	57.80	60.80	50.81	4.17	8.61	4.44

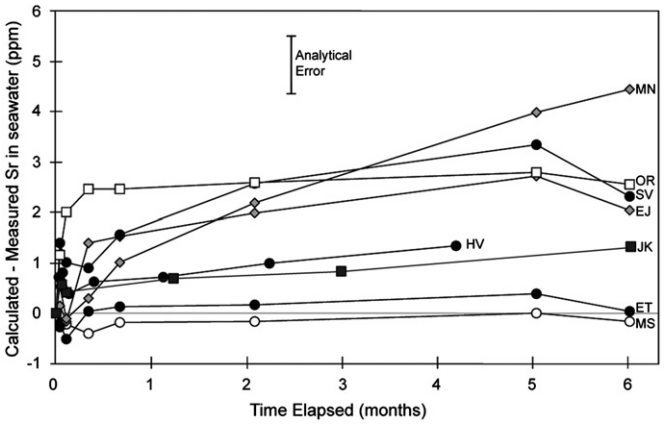

Fig. 4. A comparison of calculated Sr concentrations based on the change in $^{87}Sr/^{86}Sr$ and the measured concentrations of Sr in selected experiments. The calculated Sr values assume little or no Sr is incorporated into secondary phases. The analytical error is the sum of the errors associated with errors associated with measurement of Sr concentrations and $^{87}Sr/^{86}Sr$. The symbols match those described in Fig. 1.

with particulate dissolution. In two of the experiments this increase in Si is extreme, reaching 47 and 90 ppm in the Sveinsgil (SV) and Montserrat (MN) experiments, respectively. This is accompanied by a significant drop in pH (Table 2), suggesting that it is the acidic conditions driving these reactions. The Montserrat ash has considerable adsorbed surface salts rich in H_2SO_4 that could have caused this acidification (Jones and Gislason, 2008; Wall-Palmer et al., 2011). The Sveinsgil sample contained some pyrite, so the oxidation of Fe may have driven the change in acidity. However, there are also significant changes in Si concentrations in the experiments that do not see a large change in pH. Seawater in contact with Eyjafjallajökull (EJ) ash reaches >13 ppm Si, even though the surface coatings from that eruption are low in acidic condensate (Gislason et al., 2011) and the pH remained close to 8 (Table 2). Similarly, the samples from the Orange River (OR) and Jökulsá í Fljótsdal (JK) increased dissolved Si concentrations to 16.7 and 22.8 ppm, respectively, without a significant drop in pH.

The concentrations of Sr do not show the same degree of variation as dissolved silica (Table 2). The experiments that display the largest changes in $^{87}Sr/^{86}Sr$ also display increases in Sr concentrations. For example, in the case of the Jökulsá í Fljótsdal (JK) experiment, the large change to $^{87}Sr/^{86}Sr$ is also evident in the total Sr concentrations. Nevertheless, the increase in liquid Sr concentrations is still less than predicted from the measured changes to $^{87}Sr/^{86}Sr$ (Fig. 4), indicating that part of the Sr liberated from the solid phase is reincorporated into solids. This reincorporation is evident in all experiments (Fig. 4), and in the Montserrat ash (MN) experiment, the concentration of Sr actually decreases (Table 2). These observations corroborate the findings of Jones et al. (2012), where it was suggested that Sr release from riverine sediments is coupled with Sr precipitation in secondary phases. The most likely candidates for these secondary phases are carbonate minerals, based on phase equilibrium calculations and observed differences between river and estuarine sediments from the same catchment (Jones et al., 2012).

4. Discussion

4.1. Comparison between the experiments and the natural systems

This suite of experiments demonstrates that river transported particulates from a range of provenances can have a measureable effect on seawater chemistry, particularly the $^{87}Sr/^{86}Sr$ composition. Significant differences exist between closed-system batch reactors and the natural environment, principally the range in pH and the saturation states of minerals. In the Sveinsgil (SV) and Montserrat (MN) experiments, these effects have led to elevated dissolution of silicate material. However, as seawater reacting with sediments from Jökulsá í Fljótsdal (JK), Orange River (OR), and Eyjafjallajökull (EJ) show comparable changes in $^{87}Sr/^{86}Sr$ and Sr concentrations while maintaining a less affected pH, it is clear that Sr release is not an artifact of the experimental design. The liquid/solid ratio used here may be important for the saturation states of secondary minerals, which will affect the degree to which elements released from the solid phase are reincorporated into secondary phases. In contrast, several primary minerals will remain strongly undersaturated even at this liquid/solid ratio, especially for the volcanically derived particulates (Jones et al., 2012). Therefore, while the scale of sediment–seawater interaction may vary between these experiments and the natural environment, the results here confirm a proof of process.

4.2. Impact on oceanic $^{87}Sr/^{86}Sr$ and marine budget implications

All experiments reported in this study display compelling evidence that riverine particulate material releases a substantial amount of Sr to the oceans. This effect is masked by reincorporation of Sr into the solid phase that limits changes to Sr concentrations (Jones et al., 2012). While each experiment shows changes to seawater $^{87}Sr/^{86}Sr$ that are greatly in excess of the analytical error, there is huge variability between the samples. Two inferences can be drawn from the results of this study:

(1) Riverine particulate material from volcanic terrains is more reactive than material from continental catchments (c.f. Berner, 1992; Bluth and Kump, 1994; Wolff-Boenisch et al., 2004, 2006; Jones et al., 2011). In these experiments, the continental particulate materials, with the exception of the Orange River (OR) sample, release and/or exchange Sr quickly then appear to stabilize with the reacting liquid. In contrast, each volcanic particulate sample continues to alter the liquid $^{87}Sr/^{86}Sr$ at the end of these experiments. The degree of change is also different, with the least reactive volcanic sample releasing more Sr than the most reactive continental sample once normalized to particulate surface area (Fig. 3B).
(2) Surface area is an important component determining the extent of Sr release. The three samples that released the greatest percentage of Sr to seawater, namely the samples from Jökulsá í Fljótsdal, Sveinsgil, and Orange River (Fig. 3A), are the samples with the greatest specific surface area. Suspended material has a much higher specific surface area than bedload particulates (Louvat et al., 2008). As the mass of riverine suspended material transported to the oceans is greater than that of bedload (Walling, 2006), the average percentage of Sr released during our experiments may be significantly lower than that of the global dissolution of particulate material.

Given the apparent primary controls of mid-ocean ridge seafloor spreading and continental weathering on the ocean $^{87}Sr/^{86}Sr$ (Albarède et al., 1981; Brass, 1976; Goldstein and Jacobsen, 1987; Palmer and Edmond, 1989), changes in $^{87}Sr/^{86}Sr$ have been used to elucidate variations in these inputs over time in response to climatic and/or tectonic forcings (e.g. McArthur et al., 2001). Recent evidence has demonstrated that there is an imbalance between these sources (Davis et al., 2003; Elderfield and Schultz, 1996; Galy et al., 1999; Holland, 2005;

Vance et al., 2009). Estimates made assuming that dissolved riverine transport and mid-ocean ridge hydrothermal activity are the only ocean Sr sources suggest that the current ocean $^{87}Sr/^{86}Sr$ would evolve at a rate of 0.000425 Myr^{-1}, eight times the currently observed 0.000054 M yr^{-1} (Hodell et al., 1989; Vance et al., 2009).

There have been numerous attempts to resolve this imbalance. Recent studies proposed that enhanced chemical weathering rates of finely ground glacial products could resolve this imbalance (Vance et al., 2009). Current Sr riverine fluxes, therefore, may not be representative of the long-term inputs due to the effects of deglaciation (Krabbenhöft et al., 2010; Vance et al., 2009). Other studies proposed that subsurface weathering of volcanic islands could provide the missing source of unradiogenic Sr to close the global Sr cycle (Allègre et al., 2010). The exchange with off-axis seafloor sediments is another potential source of Sr (Butterfield et al., 2001; Elderfield and Gieskes ,1982; Elderfield et al., 1999; Mottl and Wheat, 1994), although mass balance calculations suggest that this flux will be minor in comparison to the accepted primary inputs (Davis et al., 2003). The results presented in this study suggest that the dissolution of riverine particulate material in seawater is another important component of the marine Sr cycle. The degree to which the dissolution of particulate material would close the observed ocean Sr imbalance depends on the relative reactivity and abundance of volcanic and continental riverine particulate material.

Volcanic and tectonically active islands are estimated to contribute $>45\%$ of river suspended material to the oceans (Milliman and Syvitski, 1992). Milliman and Farnsworth (2011) draw attention to the importance of wet, young and mountainous rivers to global fluxes. While comprising around 14% of the cumulative drainage basin area, the rivers that drain these terrains are estimated to transport close to 40% of the global dissolved flux and over 60% of the suspended-sediment flux. While some of the terrains included in this classification are older continental crust, such as in Taiwan and the Himalayas, the relative proportion of volcanic terrains such as south-east Asia, the Pacific ring of fire, and Iceland is considerably higher than in the other classifications. Therefore, the relative volcanic contribution to the suspended riverine flux is greater than the relative contribution to the dissolved flux.

The experiments performed in this study show that volcanic riverine particulates are more reactive in seawater than continental riverine particulates, both in the amount of change observed in $^{87}Sr/^{86}Sr$ ratios and the longevity of reactions. Coupled with the evidence that volcanically derived particulates comprise a greater proportion of the global suspended flux than the contribution to the dissolved flux (Milliman and Farnsworth, 2011), there is strong evidence to suggest that the global average $^{87}Sr/^{86}Sr$ isotopic ratio of particulate dissolution in the ocean will be considerably less than the average dissolved $^{87}Sr/^{86}Sr$ (≈ 0.71360). The degree to which the flux from riverine particulates affects the global Sr imbalance hinges on the global average $^{87}Sr/^{86}Sr$ composition. If this value is greater than that of seawater (0.70916), then this unquantified flux will exacerbate the Sr imbalance, while if it is below 0.70916 then it will help remediate the problem.

The results presented here represent a first step towards quantifying the importance of particulate material on the global Sr budget. The random nature of the particulate samples used in this study means that any use of these numbers to estimate the global flux will have significant uncertainties. Additional factors such as the weathering history and particle maturity, not specifically addressed in this study, may also play a role. However, to illustrate the possible effect particulate material dissolution would have on the global Sr cycle, we can make a first estimate of the relative contributions of volcanic and continental particulate material dissolution on the ocean Sr balance. If it is assumed that the global dissolved riverine flux of 16.5×10^{11} g (Sr) yr^{-1} (Gaillardet et al., 1999), 11.6×10^{11} g yr^{-1} of mantle derived Sr would be necessary to balance this flux (Allègre et al., 2010), of which $2.7 \pm 0.7 \times 10^{11}$ g yr^{-1} is attributed to hydrothermal and low temperature seafloor basalt alteration at mid-ocean ridges (Davis et al., 2003). Using the mean Sr release from the four continental (3.3%) and four volcanic experiments (10.6%), and assuming 45% of the riverine particulate flux is volcanically derived, would result in particulate release fluxes of 1.33 and 3.23×10^{11} g yr^{-1}, respectively. Note that these flux estimates are conservative as they are only based on the mass of Sr released during 6 months of interaction with seawater; suspended material/seawater interaction in nature may continue for longer time periods. The continental particulate flux, comprising granitic and carbonate sources, would require an additional unradiogenic sr source to balance the budget. If it is assumed that the $^{87}Sr/^{86}Sr$ of this flux is comparable to the global dissolved flux (~ 0.7136) then a further 0.93×10^{11} g yr^{-1} of mantle-like Sr to maintain balance between fluxes. This value could be significantly higher if the non-volcanic particulate flux is dominated by the radiogenic, granitic component. Despite these large uncertainties, the samples measured in this study suggest that particulate material dissolution could significantly reduce the observed disparity between radiogenic and unradiogenic sources of Sr.

Another land-to-ocean flux of unradiogenic Sr highlighted by this study is the dissolution of fresh volcanic ash, which has been shown to significantly affect the composition of seawater (e.g. Jones and Gislason, 2008). Using the best estimate of current volcanic ash production of $1.76–2.56 \times 10^{14}$ g (ash) yr^{-1} (Durant et al., 2010) and the Sr release rates of the Eyjafjallajökull and Montserrat ashes reported here results in a flux of between 1.3 and 1.9×10^{9} g (Sr) yr^{-1} if all the volcanic ash was deposited in the ocean. Therefore, this effect is likely to be minor compared to the effect of riverine particulate material dissolution on global seawater chemistry.

4.3. Evolution of oceanic $^{87}Sr/^{86}Sr$

The $^{87}Sr/^{86}Sr$ ratio in seawater can be traced through geological time as marine carbonates reflect the composition of seawater at the time of formation. This ratio has varied considerably over geological time in response to changing tectonic, volcanic, and climatic conditions (Brass, 1976; Veizer and Compston, 1974; McArthur et al., 2001). The apparent dependence of Sr release on surface area, coupled with the unusually high reactivity of the glacial sediment from Jökulsá í Fljótsdal, supports the hypothesis put forward by Vance et al. (2009) that current fluxes may not be indicative of long-term fluxes. Moreover, given recent evidence of glacial limiting of mountain heights though efficient mechanical erosion (Egholm et al., 2009; Pedersen et al., 2010), the fine grained tilling of the Tibetan/Himalayan orogeny would correlate with the observed rise in ocean $^{87}Sr/^{86}Sr$ through the late Neogene (Hodell et al., 1989) if the source was a combination of chemical weathering in situ and subsequent dissolution of mechanically weathered material. The importance of the weathering of volcanic islands to the global Sr cycle has been highlighted by Allègre et al. (2010), who suggest the poorly constrained groundwater transport of elements may close the Sr budget deficit. Our findings corroborate this significance of volcanic island weathering, but suggest that there is another substantial transport pathway available for land-to-ocean transfer of Sr. Constraining the relative contributions of these fluxes is necessary to solve the current Sr imbalance.

5. Conclusion

The dissolution of riverine particulate material in the ocean may be a significant factor in resolving the current Sr imbalance of the oceans. Although surface area, Sr concentrations, mineralogy, residence times in soils, local climate, and the degree of weathering will all be important to the subsequent behavior of riverine particulate material in seawater, the results summarized above demonstrate that riverine particulate material is a major contributor of Sr to the oceans, and any attempts at balancing the oceanic Sr budget need to include this factor to accurately describe the Sr cycle over geologic time. This conclusion is supported by a number of fundamental observations. Volcanic river suspended material is more reactive than continental river suspended material and forms a greater proportion of the global particulate flux than the dissolved flux (Milliman and Farnsworth, 2011), such that the particulate Sr flux will have a lower $^{87}Sr/^{86}Sr$ ratio than the total dissolved riverine flux. If this flux has an $^{87}Sr/^{86}Sr$ ratio below that of seawater, then it would close at least part of the current observed budget deficit. If the release rates from continental and volcanic sediments presented above are broadly representative of global fluxes, then this initial release on contact with seawater would significantly diminish the current Sr imbalance, with the flux volcanic riverine particulates predicted to be similar in magnitude to the flux predicted from hydrothermal exchange at mid-ocean ridges. This study focuses solely on the Sr cycle, but these findings of rapid particulate material–seawater exchange could conceivably apply to other elements, particularly other alkali earth metals such as Ca and Mg. As these elements are so integral to climate over geological timescales, and have calculated budgets that are not at steady state (Tipper et al., 2006; Vance et al., 2009), further work should investigate the role of riverine particulate material as a flux in these element cycles and budgets.

Acknowledgments

We thank Jerome Gaillardet and John Compton for the provision of samples. Derek Vance and an anonymous reviewer provided constructive and insightful comments and criticisms on this manuscript. M. T. Jones and C. R. Pearce were supported by the EC Marie Curie 'MIN-GRO' Research and Training Network (MRTN-CT-2006-035488). M. T. Jones is currently supported by a Marie Curie Intra-European Fellowship (PIEF-GA-2009-254495).

Appendix A. Supporting information

Supplementary data associated with this article can be found in the online version at http://dx.doi.org/10.1016/j.epsl.2012.08.040.

References

Albarède, F., Michard, A., Minster, J., Michard, G., 1981. $^{87}Sr/^{86}Sr$ ratios in hydrothermal waters and deposits from the East Pacific Rise at 21°N. Earth Planet. Sci. Lett. 55, 229–236.

Allègre, C., Louvat, P., Gaillardet, J., Meynadier, L., Rad, S., Capmas, F., 2010. The fundamental role of island arc weathering in the oceanic Sr isotope budget. Earth Planet. Sci. Lett. 292, 51–56.

Aller, R., 1998. Mobile deltaic and continental shelf muds as suboxic, fluidized bed reactors. Mar. Chem. 61, 143–155.

Aller, R.C., Blair, N.E., Brunskill, G.J., 2008. Early diagenetic cycling, incineration, and burial of sedimentary organic C in the central Gulf of Papua (Papua New Guinea). J. Geophys. Res. 113 , http://dx.doi.org/10.1029/2006JF000689, F01S09.

Arsouze, T., Dutay, J.-C., Lacan, F., Jeandel, C., 2009. Reconstructing the Nd oceanic cycle using a coupled dynamical-biogeochemical model. Biogeosciences 6, 1–18.

Berner, R.A., 1992. Weathering, plants and the long-term carbon-cycle. Geochim. Cosmochim. Acta 56, 3225–3231.

Bluth, G.J.S., Kump, L.R., 1994. Lithologic and climatologic controls of river chemistry. Geochim. Cosmochim. Acta 58, 2341–2359.

Brass, G., 1976. The variation of the marine $^{87}Sr/^{86}Sr$ ratio during Phanerozoic time: interpretation using a flux model. Geochim. Cosmochim. Acta 40, 720–730.

Broecker, W.S., Peng, T.H., 1982. Tracers in the Sea. Eldigio Press, Lamont (Doherty Geological Observatory).

Brunauer, S., Emmett, P.H., Teller, E.J., 1938. Adsorption of gases in multimolecular layers. J. Am. Chem. Soc. 60, 309–319.

Butterfield, D.A., Nelson, B.K., Wheat, C.G., Mottl, M.J., Roe, K.K., 2001. Evidence for basaltic Sr in midocean ridge-flank hydrothermal systems and implications for the global oceanic Sr isotope balance. Geochim. Cosmochim. Acta 65, 4141–4153.

Compton, J.S., Maake, L., 2007. Source of the suspended load of the upper Orange River, South Africa. S. Afr. J. Geol. 110, 339–348.

Davis, A., Bickle, M., Teagle, D., 2003. Imbalance in the oceanic strontium budget. Earth Planet. Sci. Lett. 112, 173–187.

Durant, A.J., Bonadonna, C., Horwell, C.J., 2010. Atmospheric and environmental impacts of volcanic particulates. Elements 6, 235–240.

Egholm, D.L., Nielsen, S.B., Pedersen, V.K., Lesemann, J.-E., 2009. Glacial effects limiting mountain height. Nature 460, 884–887.

Eiriksdottir, E.S., Louvat, P., Gislason, S.R., Óskarsson, N., Harðardóttir, J., 2008. Temporal variation of chemical and mechanical weathering in NE Iceland: Evaluation of a steady-state model of erosion. Earth Planet. Sci. Lett. 272, 78–88.

Elderfield, H., Gieskes, J.M., 1982. Sr isotopes in interstitial waters of marine sediments from Deep Sea Drilling Project cores. Nature 300, 493–497.

Elderfield, H., Schultz, A., 1996. Mid-ocean hydrothermal fluxes and the chemical composition of the ocean. Ann. Rev. Earth Planet. Sci. 24, 191–224.

Elderfield, H., Wheat, C.G., Mottl, M.J., Monnin, C., Spiro, B., 1999. Fluid and geochemical transport through oceanic crust: A transect across the eastern flank of the Juan de Fuca ridge. Earth Planet. Sci. Lett. 172, 151–165.

Gaillardet, J., Dupré, B., Allègre, C., 1999. Geochemistry of large river suspended sediments: silicate weathering or recycled tracers? Geochim. Cosmochim. Acta 63, 4037–4051.

Gaillardet, J., Viers, J., Dupré, B., 2003. Trace elements in river waters.. In: J.I. Drever, (Ed.). Surface and Ground Water, Weathering, and Soils, vol. 5. In: H.G. Holland, K.K. Turekian (Exec. Eds.), Treatise on Geochemistry. Elsevier.

Galy, A., France-Lanord, C., Derry, L.A., 1999. The strontium isotopic budget of Himalayan rivers in Nepal and Bangladesh. Geochim. Cosmochim. Acta 63 (13-14), 1905–1925.

Gislason, S., Oelkers, E., Snorrason, Á., 2006. Role of river-suspended material in the global carbon cycle. Geology 34, 49–52.

Gislason, S.R., Oelkers, E.H., Eiriksdottir, E.S., Kardjilov, M.I., Gisladottir, G., Sigfusson, B., Snorrason, A., Elefson, S.Ó., Hardardottir, J., Torssander, P., Oskarsson, N., 2008. Direct evidence of the feedback between climate and weathering. Earth Planet. Sc. Lett. 277, 213–222.

Gislason, S.R., Hassenkam, T., Nedel, S., Bovet, N., Eiriksdottir, E.S., Alfredsson, H.A., Hem, C.P., Balogh, Z.I., Dideriksen, K., Oskarsson, N., Sigfusson, B., Larsen, G., Stipp, S.L.S., 2011. Characterization of Eyjafjallajökull volcanic ash particles and a protocol for rapid risk assessment. Proc. Natl. Acad. Sci. U.S.A. , http://dx.doi.org/10.1073/pnas.1015053108.

Goldstein, S., Jacobsen, S., 1987. The Nd and Sr isotopic systematics of river-water dissolved material: implications for the sources of Nd and Sr in seawater. Chem. Geol. 66, 245–272.

Hodell, D., Mueller, P., McKenzie, J., Mead, G., 1989. Strontium isotope stratigraphy and geochemistry of the late Neogene ocean. Earth Planet. Sci. Lett. 92, 165–178.

Holland, H.D., 2005. Sea level, sediments and the composition of seawater. Am. J. Sci. 305, 220–239.

Hsieh, Y.-T., Henderson, G.M., Thomas, A.L., 2011. Combining 232Th and 230^{Th} concentrations to determine dust fluxes to the surface ocean. Earth Planet. Sci. Lett. 312 (3-4), 280–290.

Jeandel, C., Peucker-Ehrenbrink, B., Jones, M.T., Pearce, C.R., Oelkers, E.H., Godderis, Y., Lacan, F., Aumont, O., Arsouze, T., 2011. Ocean margins: the missing term in oceanic element budgets? EOS Trans. AGU 95 (26), 217.

Jones, M.T., Gislason, S.R., 2008. Rapid releases of metal salts and nutrients following the deposition of volcanic ash into aqueous environments. Geochim. Cosmochim. Acta 72, 3661–3680.

Jones, M.T., Hembury, D.J., Palmer, M.R., Tonge, B., Darling, W.G., Loughlin, S., 2011. The weathering and element fluxes from active volcanoes to the oceans: a Montserrat case study. Bull. Volcanol. 73, 207–222, http://dx.doi.org/10.1007/s00445-010-0397-0.

Jones, M.T., Pearce, C.R., Oelkers, E.H., 2012. An experimental study of the interaction of basaltic riverine particulate material and seawater. Geochim. Cosmochim. Acta 77, 108–120, http://dx.doi.org/10.1016/j.gca.2011.10.044.

Krabbenhöft, A., Eisenhauer, A., Böhm, F., Vollstaedt, H., Fietzke, J., Liebetrau, V., Augustin, N., Peucker-Ehrenbrink, B., Müller, M.N., Horn, C., Hansen, B.T., Nolte, N., Wallmann, K., 2010. Constraining the marine strontium budget with natural strontium isotope fractionations ($^{87}Sr/^{86}Sr*$, $d^{88/86}Sr$) of carbonates, hydrothermal solutions and river waters. Geochim. Cosmochim. Acta 74, 4097–4109.

Lacan, F., Jeandel, C., 2005. Neodymium isotopes as a new tool for quantifying exchange fluxes at the continent-ocean interface. Earth Planet. Sci. Lett. 232, 245–257.

Louvat, P., Gislason, S.R., Allègre, C.J., 2008. Chemical and mechanical erosion rates in Iceland as deduced from river dissolved and solid material. Am. J. Sci. 308, 679–726.
Mackenzie, F.T., Garrels, R.M., 1966. Chemical mass balance between rivers and oceans. Am. J. Sci. 264, 507–525.
Martin, J.-M., Meybeck, M., 1979. Elemental mass-balance of material carried by major world rivers. Mar. Chem. 7, 173–206.
McArthur, J.M., Howarth, R.J., Bailey, T.R., 2001. Strontium isotope stratigraphy: LOWES version 3: best fit to the marine Sr-isotope curve for 0-509 Ma and accompanying look-up table for deriving numerical ager. J. Geol. 109 (2), 155–170.
Meybeck, M., Laroche, L., Dürr, H., Syvitski, J., 2003. Global variability of daily total suspended solids and their fluxes in rivers. Global Planet Change 39, 65–93.
Michalopoulos, P., Aller, R.C., 1995. Rapid clay mineral formation in Amazon delta sediments: reverse weathering and oceanic elemental cycles. Science 270, 614–617.
Milliman, J., Farnsworth, K.L., 2011. River Discharge to the Coastal Ocean: A Global Synthesis. Cambridge University Press.
Milliman, J., Syvitski, J., 1992. Geomorphic/tectonic control of sediment discharge to the ocean: the importance of small mountainous rivers. J. Geol. 100, 525–544.
Milliman, J.D., 2001. River inputs. In: Steele, J.H. (Ed.), Encyclopedia of Ocean Sciences. Academic Press.
Mottl, M.J., Wheat, C.G., 1994. Hydrothermal circulation through mid-ocean ridge flanks fluxes of heat and magnesium. Geochim. Cosmochim. Acta 58, 2225–2237.
Oelkers, E.H., Gislason, S.R., Eiríksdóttir, E.S., Jones, M.T., Pearce, C.R., Jeandel, C., 2011. The role of riverine particulate material on the global cycles of the elements. Appl. Geochem. 26, S365–S369.
Palmer, M., Edmond, J., 1989. The strontium isotope budget of the modern ocean. Earth Planet. Sci. Lett. 92, 11–26.
Pearce, C.R., Burton, K.W., Pogge von Strandmann, P.A.E., James, R.H., Gislason, S.R., 2010. Molybdenum isotope behaviour accompanying weathering and riverine transport in a basaltic terrain. Earth Planet. Sci. Lett. 295, 104–114.
Pedersen, V.K., Egholm, D.L., Nielsen, S.B., 2010. Alpine glacial topography and the rate of rock column uplift: a global perspective. Geomorphology 122, 129–139.
Pogge von Strandmann, P.A.E., James, R.H., van Calsteren, P., Gislason, S.R., Burton, K.W., 2008. Lithium, magnesium and uranium isotope behaviour in the estuarine environment of basaltic islands. Earth Planet. Sci. Lett. 274, 462–471.
Peucker-Ehrenbrink, B., Miller, M.W., Arsouze, T., Jeandel, C., 2010. Continental bedrock and riverine fluxes of strontium and neodymium isotopes to the oceans. Geochem. Geophys. Geosyst. 11, Q03016, http://dx.doi.org/10.1029/2009GC002869.
Stein, M., Starinsky, A., Katz, A., Goldstein, S.L., Machlus, M., Schramm, A., 1997. Strontium isotopic, chemical, and sedimentological evidence for the evolution of Lake Lisan and the Dead Sea. Geochim. Cosmochim. Acta 61, 3975–3992.
Syvitski, J., Peckham, S., Hilberman, R., Mulder, T., 2003. Predicting the terrestrial flux of sediment to the global ocean: a planetary perspective. Sediment. Geol. 162, 5–24.
Tipper, E.T., Galy, A., Gaillardet, J., Bickle, M.J., Elderfield, H., Carder, E.A., 2006. The magnesium isotope budget of the modern ocean: constraints from riverine magnesium isotope ratios. Earth Planet. Sci. Lett. 250, 241–253.
Vance, D., Teagle, D., Foster, G., 2009. Variable quaternary chemical weathering fluxes and imbalances in marine geochemical budgets. Nature 458, 493–496.
Veizer, J., Compston, W., 1974. $^{87}Sr/^{86}Sr$ composition of seawater during the Phanerozoic. Geochim. Cosmochim. Acta 38, 1461–1484.
Viers, J., Dupré, B., Gaillardet, J., 2009. Chemical composition of suspended sediments in World Rivers: new insights from a new database. Sci. Total Environ. 407, 853–868.
Wall-Palmer, D., Jones, M.T., Hart, M.B., Fisher, J.K., Smart, C.W., Palmer, M.R., Fones, G.R., 2011. Ocean acidification from explosive eruptions as a cause for mass mortality of pteropods. Mar. Geol. 282 (3-4), 231–239.
Walling, D.E., 2006. Human impact on land–ocean sediment transfer by the world's rivers. Geomorphology 79, 192–216.
Wallmann, K., Aloisi, G., Haeckel, M., Tishchenko, P., Pavlova, G., Greinert, J., Kutterolf, S., Eisenhauer, A., 2008. Silicate weathering in anoxic marine sediments. Geochim. Cosmochim. Acta 72, 2895–2918.
Wolff-Boenisch, D., Gislason, S.R., Oelkers, E.H., Putnis, C.V., 2004. The dissolution rates of natural glasses as a function of their composition at pH 4 and 10.6, and temperatures from 25 to 74 °C. Geochim. Cosmochim. Acta 68, 4843–4858.
Wolff-Boenisch, D., Gislason, S.R., Oelkers, E.H., 2006. The effect of crystallinity on dissolution rates and CO_2 consumption capacity of silicates. Geochim. Cosmochim. Acta 70, 858–870.